Published in final edited form as:
*Clin Cancer Res*. 2009 December 1; 15(23): 7299–7308. doi:10.1158/1078-0432.CCR-09-1745.

# Targeted Drug and Gene Delivery Systems for Lung Cancer Therapy

**Sneha Sundaram**[1,2], **Ruchit Trivedi**[2], **Chandrasekar Durairaj**[2], **Rajagopal Ramesh**[3], **Balamurali K. Ambati**[4], and **Uday B. Kompella**[1,2]

[1] Department of Pharmaceutical Sciences, University of Colorado Denver, Aurora, Colorado, 80045

[2] Department of Pharmaceutical Sciences, University of Nebraska Medical Center, Omaha, Nebraska, 68198

[3] Department of Thoracic and Cardiovascular Surgery, MD Anderson Cancer Center, University of Texas, Houston, Texas

[4] Moran Eye Center, University of Utah, Salt Lake City VA Health Care System, Salt Lake City, Utah

## Abstract

**Purpose—**To evaluate the efficacy of a novel docetaxel derivative of deslorelin, a luteinizing hormone releasing hormone (LHRH) agonist, and its combination in-vivo with RGD peptide conjugated nanoparticles encapsulating an anti-angiogenic, anti-VEGF intraceptor (Flt23k) (RGD-Flt23k-NP) in H1299 lung cancer cells and/or xenografts in athymic nude BALB/c mice.

**Experimental Design—**The in-vitro and in-vivo efficacy of the deslorelin-docetaxel conjugate (D-D) was evaluated in H1299 cells and xenografts in athymic nude mice. Co-administration of D-D and RGD-Flt23k-NP was tested in-vivo in mice. Tumor inhibition, apoptosis and VEGF inhibition were estimated in each of the treatment groups.

**Results—**The conjugate enhanced in-vitro docetaxel efficacy by 13-fold in H1299 cells compared to docetaxel at 24h, and this effect was inhibited following reduction of LHRH-receptor expression by an antisense oligonucleotide. Combination of the conjugate with the RGD-Flt23k-NP in-vivo resulted in an 82- and 15-fold tumor growth inhibition on day 39 following repeated weekly intravenous injections and a single intratumoral injection, respectively. These effects were significantly greater than individual targeted therapies or docetaxel alone. Similarly, apoptotic indices for the combination therapy were 14 and 10% in the intravenous and intratumoral groups, respectively, and higher than the individual therapies. Combination therapy groups exhibited greater VEGF inhibition in both the intravenous and intratumoral groups.

**Conclusions—**Docetaxel efficacy was enhanced by LHRH-receptor targeted deslorelin conjugate and further improved by combination with targeted anti-angiogenic nanoparticle gene therapy.

Address all correspondence to: Uday B. Kompella, Department of Pharmaceutical Sciences, University of Colorado Denver, 12700 E 19th Avenue, Aurora, CO, 80045, Tel: 303-724-4028, Fax: 303-724-4666, uday.kompella@ucdenver.edu.

**TRANSLATIONAL RELEVANCE**

Cytotoxic anticancer agents such as docetaxel suffer from dose-limiting toxicities in treating lung cancer. This study advances deslorelin-docetaxel as a novel luteinizing hormone releasing hormone receptor (LHRH-R) targeted cytotoxic agent for treating lung tumors. Treatment of complex diseases such as lung cancer requires multiple therapeutic modalities. In this study, an integrin receptor targeting nanoparticulate system encapsulating an anti-VEGF intraceptor (Flt23k) plasmid has also been developed. Both targeted therapies exerted superior anti-tumor effects compared to their non-targeted counterparts in athymic nude mice bearing lung tumor xenografts. Further, combining these two targeted approaches resulted in greater lung tumor growth inhibition. Thus, targeting LHRH-receptors and integrin receptors is a viable approach in enhancing lung tumor efficacy of a cytotoxic drug and an anti-angiogenic plasmid, respectively.

Combination of novel targeted therapeutic approaches described here provides an attractive alternative to the current treatment options for lung cancer therapy.

**Keywords**

Deslorelin-docetaxel conjugate (D-D); anti-VEGF intraceptor Flt23k plasmid (Flt23k); targeted chemotherapy; lung cancer; luteinizing hormone releasing hormone receptor (LHRH-R); nanoparticles (NP)

## INTRODUCTION

Lung cancer is the leading cause of cancer related deaths worldwide (1). In 2009, an estimated 219,440 new lung cancer cases and 159,390 deaths are expected in the United States of America alone (2). Non-small cell lung cancer (NSCLC) accounts for 87 % of all cases (2,3), with a dismal 5 year survival rate of 15 % (1). Almost two-thirds (70 %) of patients present locally advanced disease or metastatic disease at the time of diagnosis (1,4) the primary treatment of choice for which is chemotherapy (5). In 2002, based on phase III clinical trial results, the US Food and Drug Administration approved the use of docetaxel in combination with cisplatin in chemotherapy naive NSCLC patients with unresectable locally advanced or metastatic disease (6). However, like other chemotherapeutics, docetaxel dosing and efficacy are limited by its undesirable side-effects including febrile neutropenia and myelosuppression (7) necessitating the development of more efficacious derivatives of docetaxel. One potential solution to increase potency and minimize non-target effects is targeting docetaxel delivery to tumors.

Conjugating ligands targeting receptors specifically expressed or over-expressed on cancer cells is an attractive technique to achieve targeting of delivery systems. Deslorelin, a nonapeptide luteinizing hormone releasing hormone (LHRH) super-agonist has a molecular weight of 1285 Da and exerts its effects via the LHRH-receptor (LHRH-R) (8,9). The LHRH-R, a member of the GPCR super family is expressed in various tissues including normal lung (10) and overexpressed on lung cancers cells (11,12). We have established that deslorelin can be conjugated to docetaxel at the hydroxyl (-OH) group in the serine moiety (amino acid 4) via a glutarate linker (13). One objective of this study was to determine whether the in-vitro and in-vivo efficacy of docetaxel can be enhanced by its conjugation to deslorelin in a lung cancer model.

Cancer therapy benefits from a multi-pronged approach. In addition to targeted cytotoxic therapy, anti-angiogenic therapies are expected to be beneficial in lung cancer therapy (14). The vascular endothelial growth factor (VEGF) a potent inducer of angiogenesis is over-expressed in 61–92 % of NSCLC patients (15). Studies have also shown that VEGF in the tumor microenvironment is capable of overcoming the effects of docetaxel, resulting in docetaxel resistance (16). Furthermore, VEGF causes impaired delivery of therapeutic agents to tumor cells (17), indicating that VEGF inhibition could improve the efficacy of anti-cancer agents. Indeed, the combination of bevacizumab (an anti-VEGF antibody) with chemotherapy has been shown to prolong progression free survival, and overall survival in NSCLC patients (18). However, treatment with bevacizumab is associated with serious side effects including, hypertension, neutropenia, bleeding, thrombocytopenia, and rashes as compared with control groups (19). Hence, new targeted strategies are required for the inhibition of VEGF expression and angiogenesis.

In this study, we investigated a targeted anti-VEGF gene therapy with an anti-VEGF intraceptor (Flt23k) based on nanoparticles with surface ligands targeting the integrin receptors. Flt23k is a recombinant construct of domains 2 and 3 of high affinity VEGF-R1 fused with endoplasmic reticulum retention signal sequence (Lysine-Aspartic acid-Glutamic acid-Leucine (KDEL))

constructed in a pTracer plasmid (20). This construct sequesters VEGF by the VEGF receptor in the endoplasmic reticulum, inhibiting VEGF secretion and the VEGF autocrine loop (20), thereby inhibiting angiogenesis (21). Thus, gene therapy with targeted Flt23k nanoparticles provides a potential alternative to existing and currently tested anti-VEGF therapies. The second objective of this study was to determine whether the efficacy of the deslorelin-docetaxel conjugate can be enhanced by a combination therapy with novel integrin receptor targeted anti-angiogenic nanoparticles (NP) encapsulating the anti-VEGF intraceptor plasmid (Flt23k-NP). A seven amino acid RGD peptide of sequence - Gly-Arg-Gly-Asp-Ser-Pro-Lys, that binds integrin receptors αvβ3 with high affinity and αvβ5 with low affinity (22,23) was used as neovasculature targeting ligand on the surface of these Flt23k-NPs (RGD-Flt23k-NP).

This is the first report of the efficacy of deslorelin-docetaxel conjugate and a novel targeted anti-VEGF intraceptor plasmid encapsulated nanoparticles in-vivo in subcutaneous H1299 cell xenograft bearing mouse model. Further, it demonstrates the advantage of combining chemo- and gene-therapies in treating cancer.

## MATERIALS and METHODS

### Chemicals

Deslorelin was a gift from Balance Pharmaceuticals, Inc. (Santa Monica, CA). Docetaxel was obtained from Chempacific (Baltimore, MD). H1299 cells were kindly provided by Dr. Pi-Wan Cheng (UNMC, NE). Cell culture materials, reagents and Lipofectin were obtained from Invitrogen (Carlsbad, CA). Chemicals for conjugation and buffers, poly (vinyl alcohol) (PVA), 3-(N-Morpholino) propanesulfonic acid (MOPS) and RGD peptide were obtained from Sigma-Aldrich (St. Louis, MO). Flt23k plasmid was a gift from Dr. Balamurali Ambati (Moran Eye Center, University of Utah, UT).

### Synthesis of Deslorelin-Docetaxel Conjugate (D-D)

D-D was synthesized, purified, and characterized as previously described (13).

### Cell Lines and Cell Culture

NSCLC cell line, H1299 was used for in-vitro and in-vivo experiments. H1299 cells were maintained under incubation in a humidified incubator under 5 % carbon dioxide in RPMI-1640 supplemented with 10 % fetal bovine serum (FBS) and 5 % glutamine 10 mM penicillin-streptomycin.

### Antiproliferative Effects of D-D in H1299 Lung Cancer Cells

Antiproliferative effects in H1299 cells were determined following a previously described method (13). H1299 cells in 96-well tissue culture plates were treated with 1–250 μg/ml of docetaxel (1.25–300 nM), 1–250 μg/ml of deslorelin (0.7–200 nM) and 1–250 μg/ml of D-D (0.19–46 nM docetaxel equivalent) in serum free medium over 24, 48 or 72 h. Medium alone, untreated cells and cells treated with approximate amounts of ethanol present in the 250 μg/ml docetaxel group were used as controls. The plates were analyzed at 540 nm to determine efficacy.

### LHRH-R Expression on H1299 Cells and the Influence of Decreased LHRH-R Expression on the Efficacy of D-D

The LHRH-R expression on H1299 cells was determined following a western blot analysis as previously described (24) following pretreatment with antisense oligonucleotides (AON) and sense oligonucleotides (SON) against LHRH-R. Pretreatment was carried out using a previously synthesized (25) and validated (11) SON and AON against LHRH-R as previously

described (11). Untreated cells were used as controls. Efficacy of D-D under decreased receptor conditions following pretreatment with AON was carried out following a previously described method (13).

### Preparation and Characterization of RGD Peptide Conjugated Flt23k Plasmid Loaded PLGA Nanoparticles (RGD-Flt23k-NP)

Nanoparticles were formulated as per a previously described method using a water/oil/water double emulsion solvent evaporation technique (26). RGD peptide was conjugated to nanoparticles using a process as described previously (26). Nanoparticles were characterized for particle size using dynamic light scattering. Particles were visualized using a scanning electron microscope (SEM) following gold coating.

### In-vivo Tumor Xenograft Studies using H1299 Cells

These studies were performed with approval and in accordance with guidelines of the Institutional Animal Care and Use Committee at the University of Nebraska Medical Center (Omaha, NE). Tumor inoculation in male athymic nude BALB/c mice (Harlan Sprague Dawley) and tumor volume measurement were carried out as previously described (13)

At 100 $mm^3$ tumor volume, treatments with docetaxel (2.5 mg/kg), D-D (2.5 mg/kg of docetaxel equivalent), Flt23k-NP (100 μg of plasmid equivalent nanoparticles), RGD-Flt23k-NP (100 μg of plasmid equivalent), D-D (2.5 mg/kg of docetaxel equivalent) plus RGD-Flt23k-NP (100 μg of plasmid equivalent) (as a single injection mixture) were administered. Treatments were administered as a single intratumoral dose (50 μl) as two 25 μl injections into two quadrants (halved at the length) of the tumor xenografts or as repeated weekly intravenous doses (100 μl) via the tail vein. PBS (vehicle) was administered intravenously as control. All animals were sacrificed and xenografts were isolated once tumor volumes in vehicle-treated mice measured 1500 $mm^3$. Immunohistochemical analyses were performed on these xenografts.

### In-vivo TUNEL Assay

Apoptotic cells in tumor tissues were detected by a terminal deoxynucleotidyl transferase-mediated nick end labeling (TUNEL) method using the DeadEnd Colorimetric kit (Promega) according to the manufacturer's instructions. Following incubation with the rTdT enzyme, the sections were developed with the 3,3′-diaminobenzidine (DAB) and images were obtained using Hitachi HV-D25 digital camera and EPIX-XCAPLite software V2.2 for windows at 10X magnification. Apoptotic indices were calculated by counting number of TUNEL positive cells/total number of cells in a field × 100. A total of 10 fields were counted in a random and blinded manner.

### Immunohistochemistry for VEGF Expression and CD31 plus TUNEL Dual Staining in Tumor Xenografts

Immunohistochemistry for VEGF was performed using a diaminobenzidine method in formaldehyde fixed/paraffin embedded sections wherein antigen retrieval was carried out with. 10 mM citrate buffer (pH = 6.0). VEGF staining was carried out by overnight incubation (4 °C) of primary goat anti-VEGF antibody (1:200 dilution) (R&D Systems, Minneapolis, MN) and secondary antibody rabbit anti-goat IgG (1:200 dilution). The sections were developed with the 3,3′-diaminobenzidine(DAB) and images were obtained using Hitachi HV-D25 digital camera and EPIX-XCAPLite software V2.2 for windows at 10X magnification.

Dual staining for CD31 and TUNEL was carried out using an immunofluorescence method. CD31 staining was carried out by overnight incubation (4 °C) of primary rabbit anti-CD31

antibody (1:200 dilution) (Abcam, Cambridge, MA), followed by Texas red labeled goat anti-rabbit IgG secondary antibody for 2 h (1:200 dilution). TUNEL staining was carried out according to manufacturer's protocol (Promega). Following incubation with the rTdT enzyme, the sections were developed with Streptavidin-FITC and confocal images were obtained with a 100x oil immersion lense on a Zeiss Axiovert 135 microscope equipped with a CARV optical module ("spinning disc confocal") and a Hamamatsu Orca (C4742-95) digital camera (6.7 × 6.7 μm of physical pixels).

### Statistical Analysis

The experiments were carried out with an n = 8 wells for MTT assays and n = 6 mice for in-vivo studies. Data in all cases are expressed as mean ± standard deviation. Comparison of mean values between different treatments was carried out using two-way analysis of variance (ANOVA) followed by Tukey's post-hoc analysis with the SPSS (version 8) software. The level of significance was set at $P < 0.05$.

## RESULTS

### Deslorelin-Docetaxel (D-D) is More Effective When Compared to Docetaxel

Antiproliferative effects and $IC_{50}$ values of D-D on H1299 cells are shown in Fig. 1A. Over periods of 24, 48 and 72 h exposure, it is observed that D-D is significantly more cytotoxic compared with docetaxel alone. Further, drugs/conjugates exhibit cytotoxicities in H1299 cells in the order: D-D > docetaxel > deslorelin at all three time points tested. The $IC_{50}$ values of the drugs based on a fit to a sigmoidal inhibitory $E_{max}$ pharmacodynamic model confirm this notion. Deslorelin did not have any cytotoxic effects on H1299 cells even at doses as high as 100 nM. $IC_{50}$ values could not be accurately determined for deslorelin since there was no measurable antiproliferative effect.

### Luteinizing Hormone Releasing Hormone Receptor (LHRH-R) Expression in H12299 Cells is Decreased by Pretreatment with AON Against LHRH-R

The expression of LHRH-R in H1299 cells following pretreatment with AON against LHRH-R is shown in Fig. 1B. H1299 cells (untreated) exhibit LHRH-R expression. Pretreatment with an AON against LHRH-R in H1299 cells caused a decrease in LHRH-R expression. The level of expression was determined by a densitometric analysis of band intensities from three separate experiments. Based on the densitometric analysis LHRH-R expression following pretreatment exhibits the order: Untreated (control) ~ SON treated > AON treated.

### Luteinizing Hormone Releasing Hormone-Receptor (LHRH-R) Contributes to the Effects of Deslorelin-Docetaxel (D-D)

The effects of decreased expression of LHRH-R on antiproliferative efficacy and $IC_{50}$ values of D-D are shown in Fig. 1C. Pretreatment with an AON against LHRH-R significantly decreased the cytotoxicity of D-D, which was not observed in SON treated groups. These results indicate that deslorelin retains its LHRH-R interactive ability when conjugated with docetaxel. Deslorelin treated groups did not exhibit any cytotoxicity in any pre-treatment group even at doses as high as 100nM. The $IC_{50}$ values for deslorelin could not be determined since there was no measurable antiproliferative effect.

**Characterization of Nanoparticles—**Nanoparticles were characterized by dynamic light scattering for three batches each of Flt23k-NP and RGD-Flt23k-NP. Flt23k-NP exhibited mean diameters of 284.92 ± 24.35 nm with a polydispersity index of 0.234 ± 0.028. RGD-Flt23k-NP exhibited a mean diameter of 291.48 ± 34.58 nm with a polydispersity index of 0.132 ±

0.023. The surface morphology of the nanoparticles using scanning electron microscopy is shown in Figure 2.

### Combination Therapy Enhances Tumor Growth Inhibition

A schematic of tumor inoculation, treatments and mechanism of action is presented in Figure 3. Treatment efficacy following intratumoral and intravenous administration are shown in Figure 4. Animals in vehicle-treated group attained a tumor volume of ~1509 ± 9 $mm^3$ on day 39 (Fig. 4A), at which time all tumors were measured and animals in various groups were sacrificed for isolation and further characterization of xenografts. Mice treated both intravenously (Fig. 4B) and intratumorally (Fig. 4C) exhibited tumor inhibition in the following order: D-D + RGD-Flt23k-NP > D-D ≥ RGD-Flt23k-NP > docetaxel ≥ Flt23k-NP ≫ PBS. Tumor growth reduction was observed in intratumoral groups until day 16 from treatment initiation, followed by an increase towards baseline over the next 23 days prior to sacrifice. No significant changes were observed in body weight and morbidity was not observed, indicating that all treatments were well tolerated.

### Combination Therapy Enhances Apoptosis in Tumor and Endothelial Cells

The treatment efficacy to induce apoptosis in the tumor cells (TUNEL assay) and endothelial cells (dual staining with CD31 and TUNEL) is shown in Figure 5. TUNEL positive cells were observed in all groups. As expected vehicle (PBS)-treated mice alone exhibited lesser TUNEL positive cells and more necrotic regions. TUNEL positive cells observed in various groups were in the following order: D-D + RGD-Flt23k-NP > D-D > docetaxel > RGD-Flt23k-NP > Flt23k-NP ≫ PBS in both intravenous (Fig. 5A) and intratumoral (Fig. 5B) groups. However, intravenous groups exhibited significantly higher TUNEL positive cells as compared with intratumoral group at all times. The above trend was also observed in apoptotic index calculated by counting the number of TUNEL positive cells (Fig. 5C). CD31 and TUNEL dual staining was assessed qualitatively in the xenograft sections (Fig. 5D). As evident, the endothelial cells exhibited apoptosis in the treated groups, with a rank order similar to that observed in the tumor cells.

### Combination Therapy Enhances Anti-VEGF Efficacy

Anti-angiogenic effect by VEGF inhibition in various treatment groups are shown in Figure 6. Immunohistochemical analysis exhibited VEGF inhibition in mice receiving treatments as compared with vehicle-treated mice alone. However, groups treated with Flt23k-NP, RGD-Flt23k-NP, and D-D + RGD-Flt23k-NP exhibited greater VEGF inhibition as compared with groups receiving docetaxel or D-D. VEGF inhibition was in the order: D-D + RGD-Flt23k-NP > RGD-Flt23k-NP > Flt23k-NP > D-D > docetaxel > PBS. The same trend was observed in mice treated both intravenously (Fig. 6A) as well as intratumorally (Fig. 6B). However, VEGF inhibition was higher in intravenous groups as compared with intratumoral groups.

## DISCUSSION

By employing a novel deslorelin-docetaxel conjugate (D-D) and RGD conjugated Flt3k anti-VEGF intraceptor plasmid loaded biodegradable nanoparticles (RGD-Flt23k-NP) for lung cancer therapy (Fig. 3), we report the following key findings. 1) Deslorelin-docetaxel (D-D), a targeted chemotherapeutic agent, exerts better in vitro and in-vivo cytotoxic effects compared to docetaxel alone, likely by targeting the receptors for luteinizing hormone releasing hormone. 3) RGD-Flt23k-NP, a targeted nanoparticle gene delivery system, improves in-vivo therapeutic efficacy compared to non-targeted nanoparticles of the anti-VEGF intraceptor plasmid. 4) Combination therapy of D-D, a targeted chemotherapeutic agent, with RGD-Flt23k-NP, a targeted nanoparticle anti-angiogenic agent, provides enhanced anti-tumor efficacy compared to individual therapies or docetaxel alone.

Our antiproliferative studies showed that D-D is significantly more cytotoxic compared with docetaxel alone after 24, 48, or 72 h exposure, with D-D being 10–13-fold more potent compared to docetaxel. The IC50 of D-D was as low as 0.8 nM after 72 h exposure to H1299 cells. Deslorelin by itself did not exhibit any cytotoxic effects in H1299 cells, which is consistent with our previous studies in prostate cancer cells (13).

Deslorelin, an LHRH agonist exerts its pharmacological effects via the LHRH-R (12). Our western blot analysis confirms expression of LHRH-R in H1299 similar to LNCaP and PC-3, prostate cancer cell lines, suggesting that D-D can exert its effects via LHRH-R in H1299 cells. The AON against LHRH-R significantly reduced LHRH-R expression by ~2-fold and the potency of D-D by 3.5-fold at the end of 72 h drug exposure in H1299 cells. Thus, D-D likely exerted its effects in H1299 cells, partly via an LHRH-R mediated uptake of the conjugate. Our prior studies indicated that deslorelin undergoes cellular uptake and transport via LHRH receptors (11,27,28). Thus, our in vitro studies suggest that lower doses of conjugate can achieve the same effect as docetaxel alone. Thus, the conjugate at doses comparable to docetaxel clinical doses might achieve greater tumor reductions.

Although intravenous injections are more common clinically, itratumoral injections are expected to localize and retain the dose better than intravenous injections. Therefore, we assessed a single intratumoral injection and repeated weekly intravenous injections in this study. Weekly intravenous administrations of D-D improved tumor inhibition by ~40% at the end of the study, compared to equivalent docetaxel therapy. Single intratumoral administration, on the other hand, resulted in a significant, ~20% greater tumor inhibition at the end of the study, compared to equivalent docetaxel therapy. Thus, D-D is significantly more effective compared to docetaxel. This enhanced tumor reduction, while interesting, warrants the use of additional approaches for further inhibiting lung tumor growth. Therefore, we assessed the usefulness of an anti-angiogenic therapy by itself or in combination with D-D cytotoxic therapy.

Targeted anti-VEGF gene therapies are expected to be significantly safer compared to currently available VEGF antibody therapies. Polymeric nanoparticles are effective carriers of macromolecules, protecting against macromolecule degradation in blood and/or tissues (29). Therefore, we designed integrin receptor targeted polymeric nanoparticles (Flt23k-NP) encapsulating the anti-VEGF intraceptor plasmid (Flt23k) (20). The RGD-Flt23k-NP exhibited ~30% and ~20% greater, statistically significant, tumor inhibition compared with Flt23k-NP alone in the intravenous and intratumoral groups, respectively.

Since cytotoxic and anti-angiogenic approaches treat different aspects of tumor progression, a combination of these two approaches might provide an additive effect. Therefore, we tested a combination of D-D and RGD-Flt23k-NP in-vivo. It is noteworthy that following weekly intravenous injections, D-D + RGD-Flt23k-NP achieved 82-fold tumor inhibition compared to 38-, 36-, 50-, and 46-fold growth inhibition achieved by docetaxel, Flt23k-NP, D-D, RGD-Flt23k-NP, respectively, when compared to tumor size in vehicle-treated group on day 39 after dose initiation. At this time, all intravenous treated groups maintained the tumor size below the baseline (~100 $mm^3$) by 60% or better. On the other hand, following a single intratumoral injection, the intratumoral combination therapy with D-D and RGD-Flt23k-NP resulted in a -6% tumor volume compared to the baseline. These effects were superior to intratumoral docetaxel and Flt23k-NP, the non-targeted counterparts.

The TUNEL assay suggested that D-D + RGD-Flt23k-NP achieved ~170% and ~100% greater apoptosis compared to Flt23k-NP and RGD-Flt23k-NP respectively, in both the intravenous and intratumoral groups. Further, the D-D + RGD-Flt23k-NP co-administration achieved a ~50%, and ~30% greater apoptosis compared to docetaxel and D-D respectively, in both the

intravenous and intratumoral groups. D-D enhanced apoptosis by ~30% compared to docetaxel alone in both the intravenous and intratumoral treated groups. Flt23k-NP treated groups also exhibited greater apoptosis compared to the vehicle-treated groups, which increased further by ~40% when treated with RGD-Flt23k-NP. In addition to the above measures for apoptosis in tumor tissue at the end of the study, we also assessed apoptosis in endothelial cells of the tumor vasculature. The qualitative rank order for apoptosis in endothelial cells was similar to what was observed above in tumor cells, with the combination therapy exhibiting the highest apoptotic activity. While the above observed apoptotic activity of docetaxel is well known, it is interesting to note that Flt23k plasmid, capable of inhibiting VEGF secretion (20), also resulted in apoptotic activity. There is some evidence indicating that inhibition of VEGF leads to apoptosis (14). Bevacizumab administered intraperitoneally inhibits tumor growth of lung adenocarcinoma xenografts by approximately 20% and leads to an increase in pro-apoptotic gene expression (30). Inhibition of VEGF is postulated to inhibit tumor growth and induce apoptosis via loss of an hitherto unidentified endothelial cell derived paracrine factor as a result of vessel regression (31,32) or due to a direct interaction between VEGF and the tumor cell itself (14).

In this study, all tumor xenografts exposed to Flt23k plasmid treatments exhibited a significant VEGF inhibition at the end of the study. We also observed that VEGF inhibtion was also increased in the D-D groups. The highest VEGF inhibition was evident in the D-D + RGD-Flt23k-NP group, possibly due to VEGF inhibition by both docetaxel as well as the anti-VEGF intraceptor. Previous studies have shown that docetaxel itself can lead to VEGF inhibition (33). Docetaxel is known to inhibit VEGF in colorectal carcinoma cells (34). However, docetaxel by itself did not inhibit VEGF in the current study, possibly due to low drug levels at the end of the study. Docetaxel, a small molecule, might have been cleared to a large extent by the end of the study (day 39) after single intratumoral injections. In intravenous injection groups, 5 days elapsed between last injection and the time of sacrifice. Docetaxel concentrations present in tumor tissue at this time might not have been adequate to inhibit VEGF. Furthermore, docetaxel at 10 mg/kg achieves only a slight VEGF inhibition (35). We have used only 2.5 mg/kg dose which is equivalent to the human dose, which likely is not adequate to observe VEGF inhibition as observed with D-D. With D-D, greater drug delivery or drug retention is anticipated. Possibly for this reason, D-D induced apoptosis as well as VEGF inhibition.

The intravenous administration differentiated targeted systems much better compared to intratumoral administration. Overall repeated intravenous administrations of treatments were able to sustain tumor volumes well below baseline compared to single intratumoral administration of treatments. The higher efficacy following intravenous injection compared to intratumoral injections could be attributed to the frequent dosing and 6-fold greater overall dose administered in the intravenous groups. Our studies suggest that targeted chemo- and anti-angiogenic gene delivery systems are both more effective approaches as compared to non-targeted delivery systems for lung cancer treatment. Further, a combination of targeted chemo- and anti-angiogenic therapy is superior to individual therapies. The assessed targeting features likely improve localization of the treatments to the tumor compared to non-targeted systems. The relative advantage of targeted systems even after intratumoral administration suggests better uptake and/or retention of targeted systems at the tumor site compared to non-targeted systems.

In conclusion, conjugation with deslorelin enhances anticancer activity of the clinically used chemotherapeutic agent docetaxel in vitro and in-vivo in lung cancer models. Further, combination of deslorelin-docetaxel with targeted anti-VEGF intraceptor gene therapy offers additive effects in inhibiting tumor growth and enhancing apoptotic index. Thus, this study

advances novel targeted chemotherapeutic and anti-angiogenic agents based on nanomaterials for cancer therapy.

## Acknowledgments

We thank Dr. Vidhya Rao for her critical input and assistance in preparation of this manuscript. We thank the American Heart Association for predoctoral fellowship award to Ms. Sneha Sundaram. We thank Drs. Rakesh Singh and Seema Singh of University of Nebraska Medical Center for their input and assistance in immunohistochemical analyses. We thank Dr. Natalia Varaksa and the NCF facility at the Univeristy of Colorado Boulder for assistance with electron microscopy.

## References

1. Molina JR, Yang P, Cassivi SD, Schild SE, Adjei AA. Non-small cell lung cancer: epidemiology, risk factors, treatment, and survivorship. Mayo Clin Proc 2008;83:584–94. [PubMed: 18452692]
2. Jemal A, Siegel R, Ward E, et al. Cancer statistics. CA Cancer J Clin 2008;58:71–96. [PubMed: 18287387]
3. Cancer Facts and Figures. American Cancer Society 2008.
4. Stinchcombe TE, Socinski MA. Considerations for second-line therapy of non-small cell lung cancer. Oncologist 2008;13 (Suppl 1):28–36. [PubMed: 18263772]
5. Pfister DG, Johnson DH, Azzoli CG, et al. American Society of Clinical Oncology treatment of unresectable non-small-cell lung cancer guideline: update 2003. J Clin Oncol 2004;22:330–53. [PubMed: 14691125]
6. Shepherd FA, Dancey J, Ramlau R, et al. Prospective randomized trial of docetaxel versus best supportive care in patients with non-small-cell lung cancer previously treated with platinum-based chemotherapy. J Clin Oncol 2000;18:2095–103. [PubMed: 10811675]
7. Vaishampayan U, Hussain M. Update in systemic therapy of prostate cancer: improvement in quality and duration of life. Expert Rev Anticancer Ther 2008;8:269–81. [PubMed: 18279067]
8. Coy DH, Coy EJ, Vilchez-Martinez JA, de la Cruz A, Arimura A, Schally AV. Suppression of gonadotropin release and ovulation in animals by inhibitory analogs of luteinizing hormone-releasing hormone. Curr Top Mol Endocrinol 1976;3:339–54. [PubMed: 802656]
9. Sundaram S, Bontha S, Kompella UB. Respiratory delivery of deslorelin, a peptide drug. Am Pharm Rev 2004;7:130–9.
10. Tieva A, Stattin P, Wikstrom P, Bergh A, Damber JE. Gonadotropin-releasing hormone receptor expression in the human prostate. Prostate 2001;47:276–84. [PubMed: 11398175]
11. Koushik K, Bandi N, Sundaram S, Kompella UB. Evidence for LHRH-receptor expression in human airway epithelial (Calu-3) cells and its role in the transport of an LHRH agonist. Pharm Res 2004;21:1034–46. [PubMed: 15212170]
12. Kakar SS, Jennes L. Expression of gonadotropin-releasing hormone and gonadotropin-releasing hormone receptor mRNAs in various non-reproductive human tissues. Cancer Lett 1995;98:57–62. [PubMed: 8529206]
13. Sundaram S, Durairaj C, Kadam R, Kompella UB. Luteinizing hormone-releasing hormone receptor-targeted deslorelin-docetaxel conjugate enhances efficacy of docetaxel in prostate cancer therapy. Mol Cancer Ther 2009;8:1655–65. [PubMed: 19509261]
14. Harmey JH, Bouchier-Hayes D. Vascular endothelial growth factor (VEGF), a survival factor for tumour cells: implications for anti-angiogenic therapy. Bioessays 2002;24:280–3. [PubMed: 11891765]
15. Fontanini G, Vignati S, Boldrini L, et al. Vascular endothelial growth factor is associated with neovascularization and influences progression of non-small cell lung carcinoma. Clin Cancer Res 1997;3:861–5. [PubMed: 9815760]
16. Sweeney CJ, Miller KD, Sissons SE, et al. The antiangiogenic property of docetaxel is synergistic with a recombinant humanized monoclonal antibody against vascular endothelial growth factor or 2-methoxyestradiol but antagonized by endothelial growth factors. Cancer Res 2001;61:3369–72. [PubMed: 11309294]

17. Lee CG, Heijn M, di Tomaso E, et al. Anti-Vascular endothelial growth factor treatment augments tumor radiation response under normoxic or hypoxic conditions. Cancer Res 2000;60:5565–70. [PubMed: 11034104]

18. Sandler A, Gray R, Perry MC, et al. Paclitaxel-carboplatin alone or with bevacizumab for non-small-cell lung cancer. N Engl J Med 2006;355:2542–50. [PubMed: 17167137]

19. Sandler AB. Advanced non-small-cell lung cancer: new data, therapy choices, and challenging decisions. Oncology (Williston Park) 2006;20:626–8. [PubMed: 16773846]

20. Singh N, Amin S, Richter E, et al. Flt-1 intraceptors inhibit hypoxia-induced VEGF expression in vitro and corneal neovascularization in vivo. Invest Ophthalmol Vis Sci 2005;46:1647–52. [PubMed: 15851564]

21. Yla-Herttuala S. Vascular gene transfer. Curr Opin Lipidol 1997;8:72–6. [PubMed: 9183544]

22. Kumar S, Li C. Targeting of vasculature in cancer and other angiogenic diseases. Trends Immunol 2001;22:129. [PubMed: 11334027]

23. Vogel BE, Lee SJ, Hildebrand A, et al. A novel integrin specificity exemplified by binding of the alpha v beta 5 integrin to the basic domain of the HIV Tat protein and vitronectin. J Cell Biol 1993;121:461–8. [PubMed: 7682219]

24. Sundaram S, Roy SK, Kompella UB. Differential expression of LHRH-receptor in bovine nasal tissue and its role in deslorelin delivery. Peptides 2009;30:351–8. [PubMed: 18992782]

25. Seong JY, Kang SS, Kam K, et al. Differential regulation of gonadotropin-releasing hormone (GnRH) receptor expression in the posterior mediobasal hypothalamus by steroid hormones: implication of GnRH neuronal activity. Brain Res Mol Brain Res 1998;53:226–35. [PubMed: 9473680]

26. Sundaram S, Roy SK, Ambati BK, Kompella UB. Surface-functionalized nanoparticles for targeted gene delivery across nasal respiratory epithelium. Faseb J. 2009

27. Kompella UB, Sundaram S, Raghava S, Escobar ER. Luteinizing hormone-releasing hormone agonist and transferrin functionalizations enhance nanoparticle delivery in a novel bovine ex vivo eye model. Mol Vis 2006;12:1185–98. [PubMed: 17102798]

28. Koushik KN, Kompella UB. Transport of deslorelin, an LHRH agonist, is vectorial and exhibits regional variation in excised bovine nasal tissue. J Pharm Pharmacol 2004;56:861–8. [PubMed: 15233864]

29. Raghava, S.; Goel, G.; Kompella, UB. Ophthalmic Applications of Nanotechnology. New York: Humana Press; 2008.

30. Inoue S, Hartman A, Branch CD, et al. mda-7 In combination with bevacizumab treatment produces a synergistic and complete inhibitory effect on lung tumor xenograft. Mol Ther 2007;15:287–94. [PubMed: 17235306]

31. Holmgren L, O'Reilly MS, Folkman J. Dormancy of micrometastases: balanced proliferation and apoptosis in the presence of angiogenesis suppression. Nat Med 1995;1:149–53. [PubMed: 7585012]

32. O'Reilly MS, Holmgren L, Chen C, Folkman J. Angiostatin induces and sustains dormancy of human primary tumors in mice. Nat Med 1996;2:689–92. [PubMed: 8640562]

33. Avramis IA, Kwock R, Avramis VI. Taxotere and vincristine inhibit the secretion of the angiogenesis inducing vascular endothelial growth factor (VEGF) by wild-type and drug-resistant human leukemia T-cell lines. Anticancer Res 2001;21:2281–6. [PubMed: 11724283]

34. Guo XL, Lin GJ, Zhao H, et al. Inhibitory effects of docetaxel on expression of VEGF, bFGF and MMPs of LS174T cell. World J Gastroenterol 2003;9:1995–8. [PubMed: 12970892]

35. Niwa H, Wentzel AL, Li M, Gooding WE, Lui VW, Grandis JR. Antitumor effects of epidermal growth factor receptor antisense oligonucleotides in combination with docetaxel in squamous cell carcinoma of the head and neck. Clin Cancer Res 2003;9:5028–35. [PubMed: 14581378]

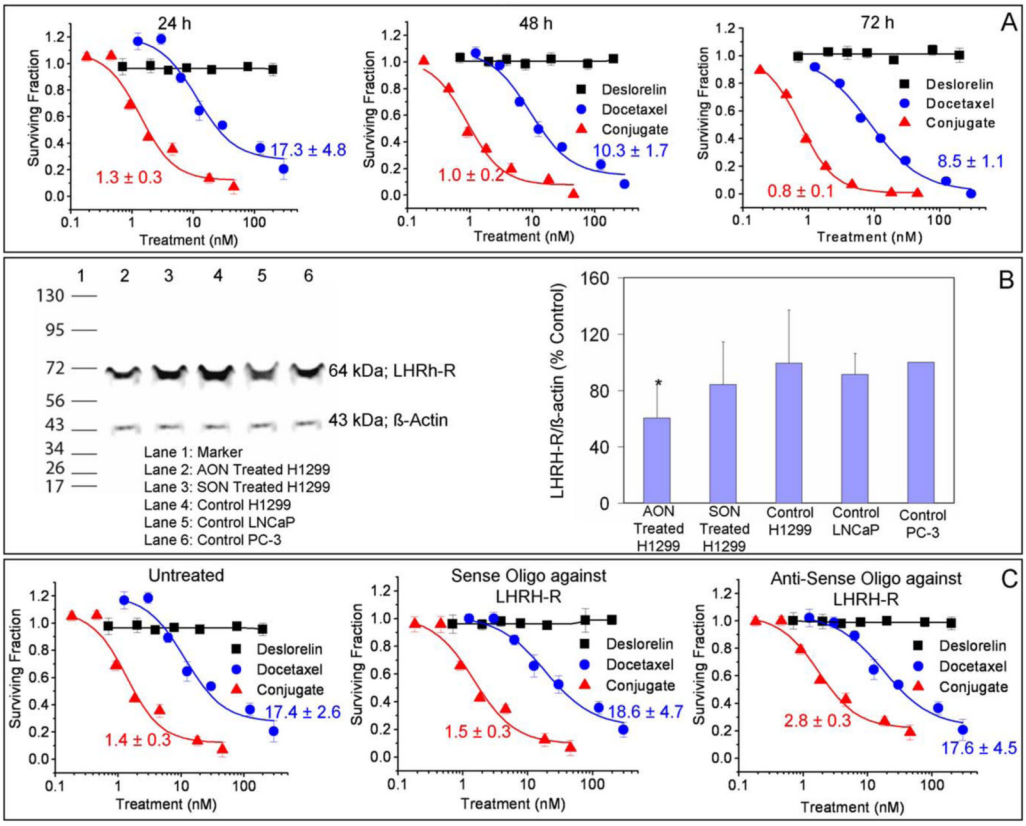


**Figure 1.**

In-vitro assessment of antiproliferative effects of deslorelin-docetaxel conjugates in H1299 lung cancer cells. A) Time course of antiproliferative effects over 24, 48 or 72h. B) Expression of LHRH-receptor – a Western blot analysis. Lane 2 represents AON treated H1299, Lane 3 represents SON treated H1299, Lane 4–6 represents control H1299, LNCaP and PC-3 cells respectively. The bands at 64 kDa represent the LHRH-R while those at 43 kDa represent internal protein standard, β-actin. The densitometric analysis of the band intensities of LHRH-receptor vs. β-actin (internal standard) are presented as mean ± standard deviation for n = 3 experiments. *P < 0.05 compared with all other groups. C) Cells pretreated with SON and AON followed by treatment with various concentrations of deslorelin, docetaxel and deslorelin-docetaxel conjugates for 24h. Data are expressed as mean ± standard deviation for n = 6. The $IC_{50}$ values were calculated using the inhibitory sigmoid $E_{max}$ model. The lines were fit using this model.

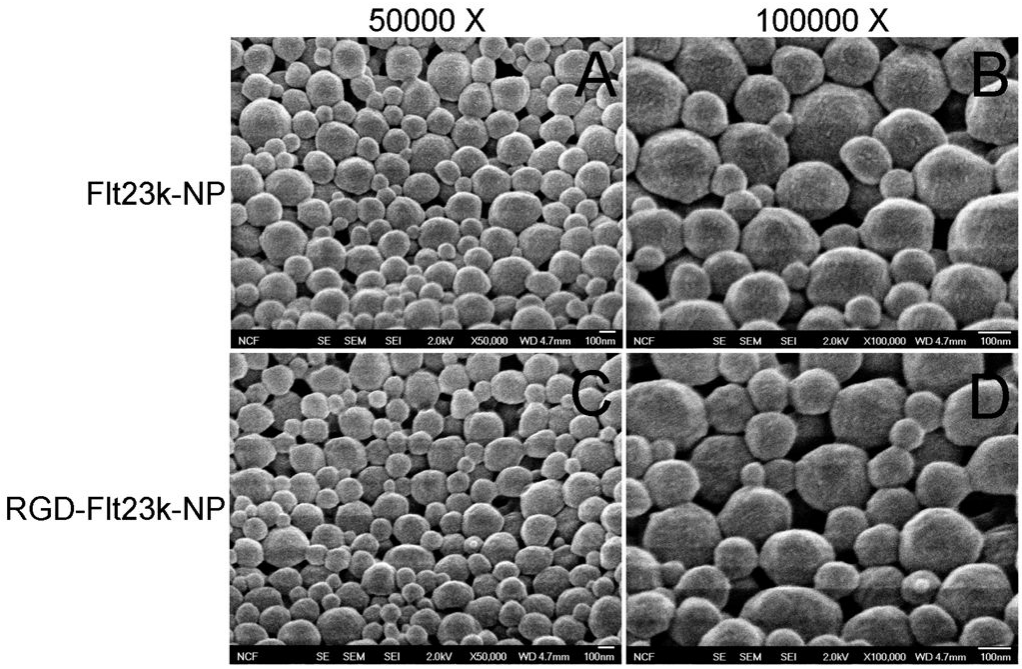


**Figure 2.**
Surface morphology of nanoparticles. Key: A and B) Flt23k-NP; C and D) RGD-Flt23k-NP. Panels A and C were obtained at a magnification of 50,000X while panels B and D were obtained at a magnification of 100,000X.

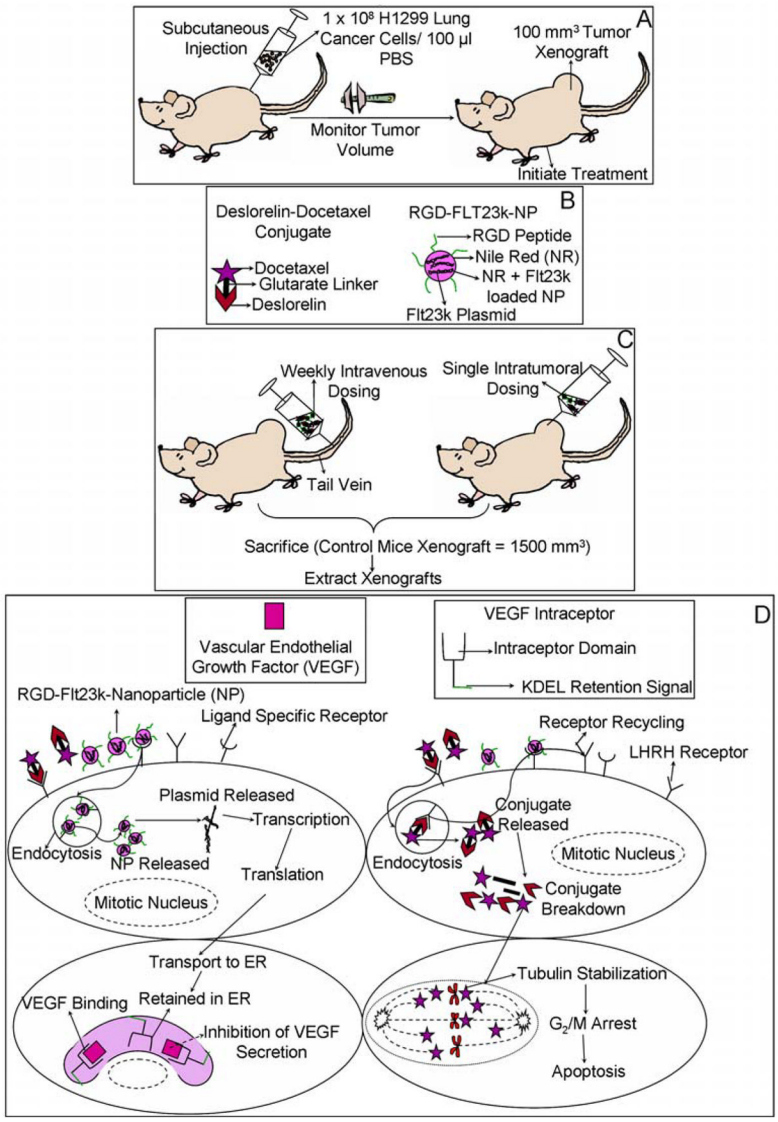


**Figure 3.**

A) Initiation of H1299 lung adenocarcinoma xenografts in athymic nude mice for assessing in-vivo pharmacological efficacy of various treatments. B) Novel targeted drug delivery systems used for treatments. C) Novel treatments in mice bearing H1299 lung adenocarcinoma xenografts. Various treatments including docetaxel, deslorelin-docetaxel conjugates (D-D), Flt23k-NP, RGD-Flt23k-NP and a combination of D-D + RGD-Flt23k-NP were administered either as repeated weekly intravenous injections or a single intratumoral injection. D) Mechanism of action of D-D and RGD-Flt23k-NP in H1299 lung adenocarcinoma xenograft bearing mice. The delivery systems are taken up by cells via receptor mediated mechanisms. The NPs release the plasmid and the VEGF intraceptor is transcribed, translated and transported to the endoplasmic reticulum. The VEGF intraceptor sequesters and ultimately inhibits VEGF secretion. D-D is endocytosed and expected to breakdown to its parent components within cells. In the tumor cells, docetaxel leads to stabilization of tubulins in spindle fibers leading to a $G_2$/M phase arrest, ultimately causing apoptosis.

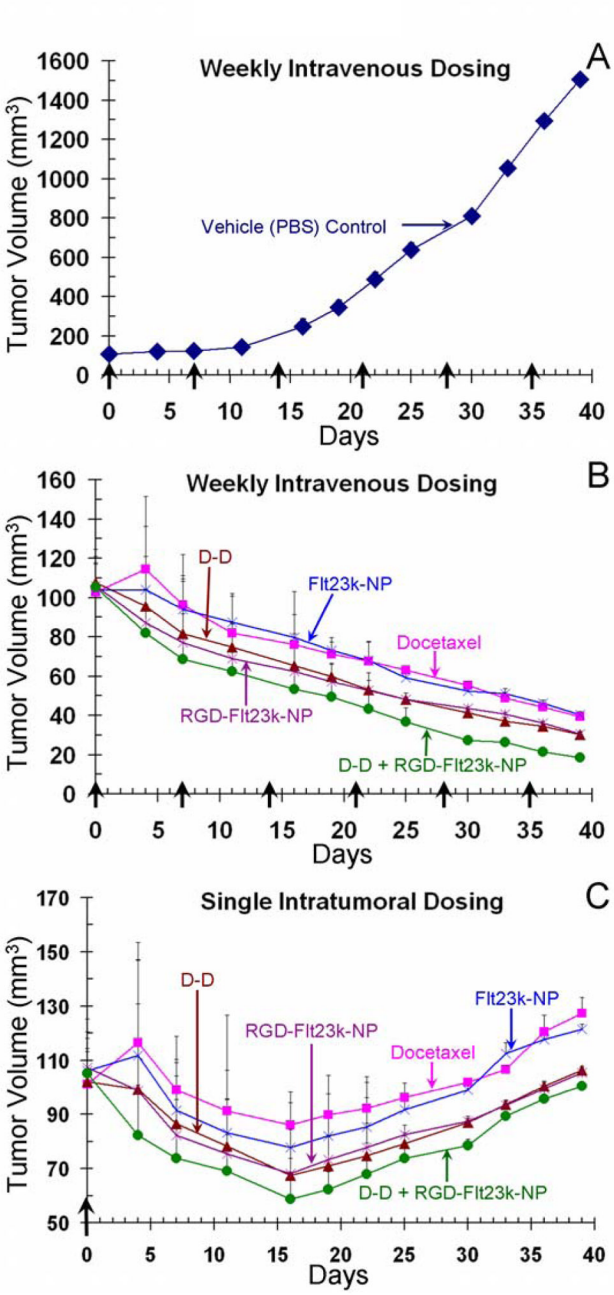


**Figure 4.**

In-vivo efficacy assessment of various treatments in H1299 lung cancer xenografts in mice. Key: A) Vehicle control (PBS); B) weekly intravenous treatment; and C) single intratumoral treatment. The mice were administered with docetaxel, deslorelin-docetaxel conjugate (D-D), Flt23k-NP, RGD-Flt23k-NP, or D-D + RGD-Flt23k-NP either intravenously or intratumorally. Control groups received PBS alone intravenously. The solid arrows and days indicate the days when intravenous treatments were administered. Data are expressed as mean ± standard deviation for n = 6 mice.

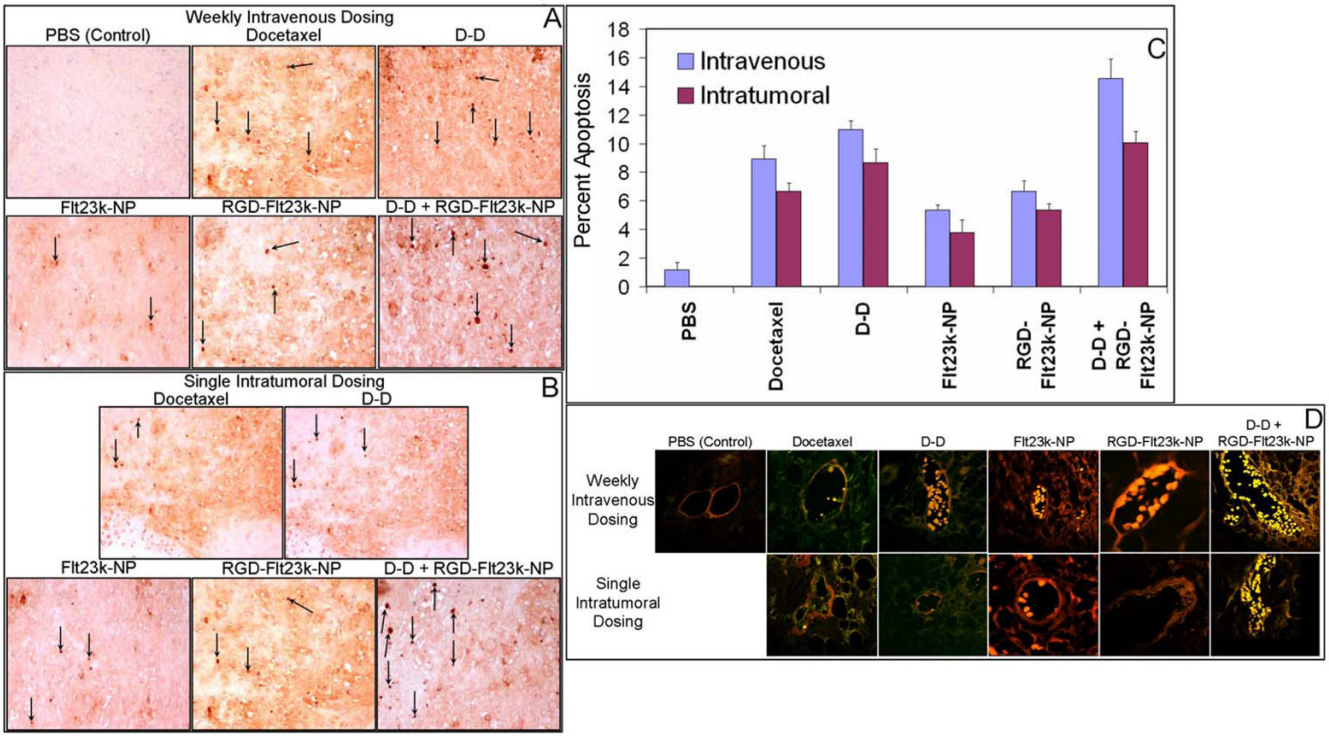


**Figure 5.**

In-vivo assessment of apoptotic efficacy of various treatments in H1299 lung cancer xenografts in mice. Representative photomicrographs of apoptotic cells in A) intravenous and B) intratumoral groups using TUNEL assay in one representative section out of n = 6 xenografts. C) The apoptotic index following intravenous and intratumoral treatments with docetaxel, D-D, Flt23k-NP, RGD-Flt23k-NP, D-D + RGD-Flt23k-NP. The arrows indicate some TUNEL positive cells in a field. Data are expressed as mean ± standard deviation for n = 6. D) Representative photomicrographs of apoptosis in proliferative endothelial cells using a dual CD31 and TUNEL staining in one representative section out of 6 xenografts.

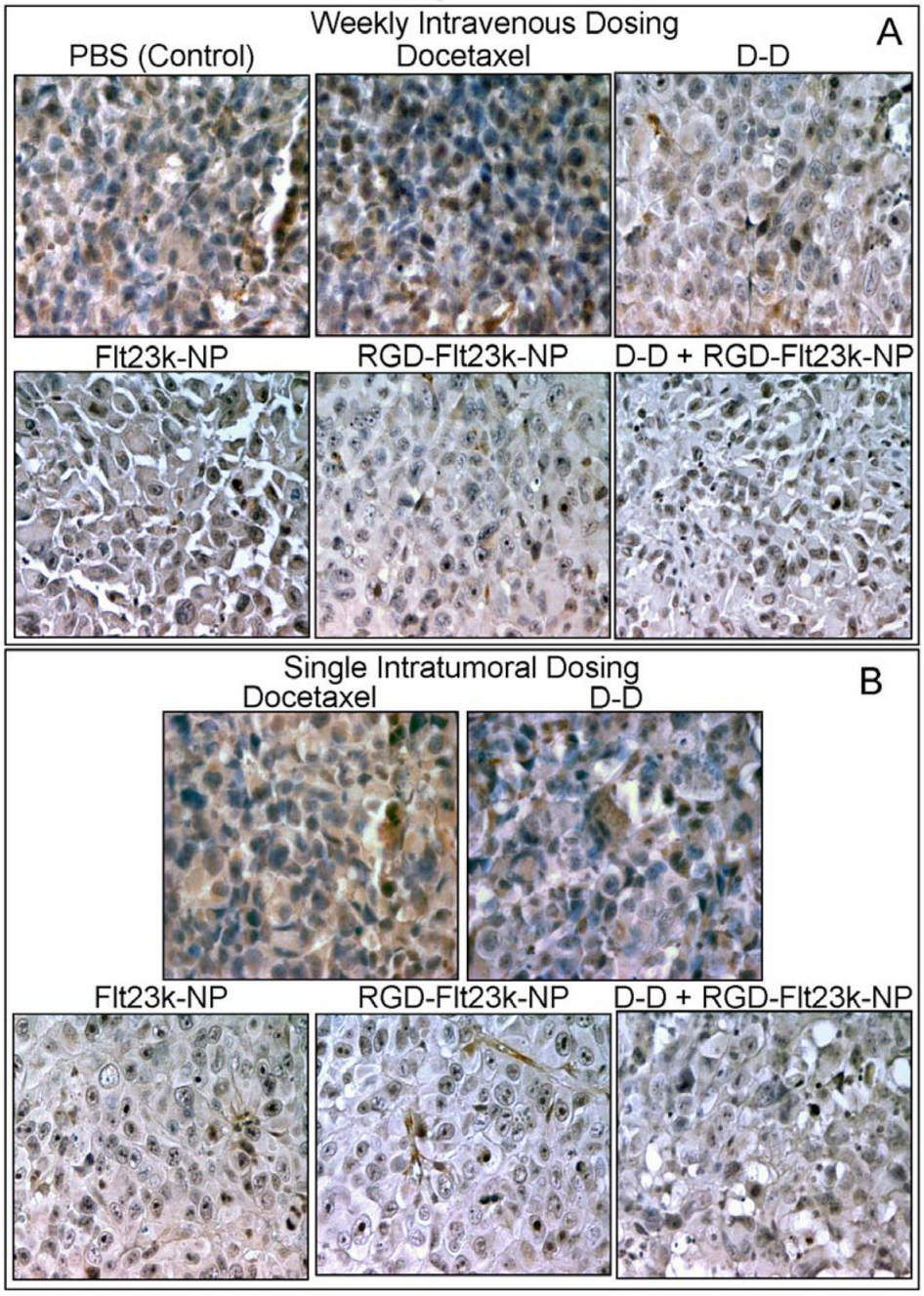


**Figure 6.**

In-vivo assessment of efficacy of various treatment groups in inhibiting VEGF expression in H1299 lung cancer xenografts models. Representative photomicrographs of VEGF expression (brown stain) using a VEGF immunohistochemistry assay in A) intravenous and B) intratumoral groups following various treatments including docetaxel, D-D, Flt23k-NP, RGD-Flt23k-NP, and D-D + RGD-Flt23k-NP. These are representative of sections in one out of 6 xenografts.